

## PRELIMINARY INVESTIGATION OF THE SHEAR FRICTION CAPACITY OF INTERFACES WITHOUT STEEL CROSSING THE INTERFACE

**Fatima C. Vieira, MS**, Florida International University, Miami, FL.

**Bruno R. Vasconcelos, PE**, Florida Department of Transportation, Tallahassee, FL.

**David Garber, PhD, PE**, Dep. of Civil Engineering, Florida International University, Miami, FL.

### ABSTRACT

*Prefabricated Bridge Elements and Systems (PBES) are being more widely used, as they can significantly reduce on-site construction time impacting traffic. The main concerns when using PBES are the final assembly of the elements, type of connection between them, and tolerance to allow for field fit up. The Florida Department of Transportation (FDOT) currently recommends a pocket connection detail between the precast pile cap and precast pile, which relies on the bearing strength between the end of the pile and pile cap and the shear friction capacity between the CIP plug and the precast cap. Current code expressions for shear friction include components for cohesion or aggregate interlock and a contribution from steel crossing the interface or a clamping force, but were developed primarily on the basis of shear friction tests with steel crossing the interface. A numerical analysis was conducted to evaluate the failure mechanism and the shear friction capacity of the plane between the precast pile cap and CIP plug. An experimental investigation was conducted on several specimens to verify the numerical results and explore experimentally the behavior of this interface. Results from the numerical and experimental work will be discussed in this presentation.*

**Keywords:** Pre-cast Concrete, Substructure Connection, Shear Friction.

## INTRODUCTION

Prefabricated Bridge Element and Systems (PBES) are being more widely used, as they can dramatically reduce on-site construction time impacting traffic. The main concerns when using PBES are the on-site final assembly of the elements, tolerance allowances, and the type of connection used between elements.

Current code expressions for shear friction include components for cohesion or aggregate interlock as well as a contribution from steel crossing the interface or clamping force. These expressions were developed primarily based on shear friction tests with steel crossing the interface. The main objective of this project is to evaluate the connection detail between precast pile caps and precast piles without steel crossing the interface. This connection relies on the shear friction capacity of the interface, which is a behavior that has not been appropriately studied.

The principal objective of this paper is to discuss previously conducted tests to evaluate the shear friction capacity, the current recommended equations and connection details between precast pile caps and precast piles, as well as preliminary experimental evaluations from small-scale specimens that were tested to evaluate the capacity of interfaces without steel crossing the shear plane.

## SHEAR FRICTION

### BACKGROUND

Shear friction is a term used to describe the shear transfer mechanism along an interface between two concrete members that were cast at different times or two adjacent members that can slip relative to each other<sup>1</sup>. Shear friction is typically critical either at cold joints or geometric discontinuities. Some examples of shear friction in practice include<sup>2</sup>:

- Repairing or strengthening an existing reinforced concrete member through adding new concrete layers;
- Supplementing precast elements with concrete cast on the site;
- Casting new concrete against concrete that has been completely hardened because the erection process was interrupted;
- Post-installations of concrete elements attached to existing members for introduction of loads; and
- Field connection of precast elements using cast-in-place concrete connections.

Some of these examples found in practice are shown in Fig 1.

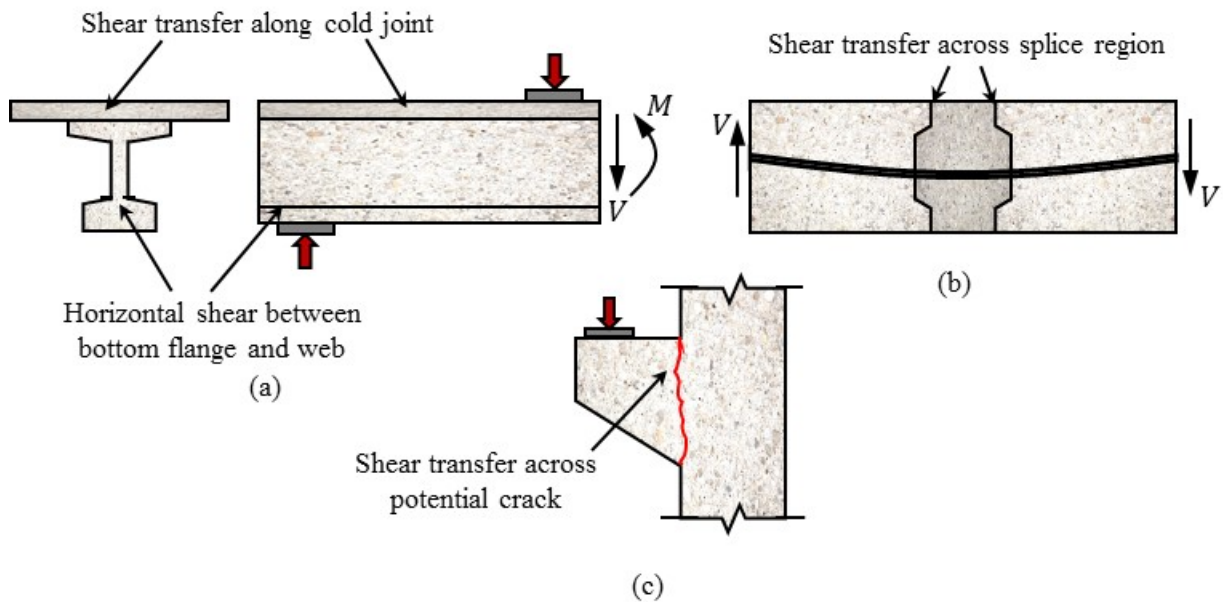


Fig 1: Example of shear friction in (a) composite girder, (b) splice region (or other joint between pre-cast members), and (c) corbel.

### SHEAR FRICTION COMPONENTS

The principal components that contributes to the shear friction capacity are:

- Cohesion or aggregate interlock,
- Friction,
- Reinforcement crossing the interface,
- Concrete strength and curing conditions

The effects of cohesion and friction in the interface are directly related to the surface preparation and surface roughness. The bond strength between the materials at the joint is achieved by having a higher degree of roughness on the interface surface<sup>3</sup>. The use of modern technologies to prepare the surface has allowed for more consistently achieving the desirable roughness. Some of these technologies are: high-pressure water-jetting (HPW), milling, shot-blasting or sand-blasting<sup>4</sup>. A paste retarder can also be painted on formwork to create an exposed aggregate finish with increased surface roughness.

Reinforcement crossing the interface plays two important roles when transmitting stresses between interfaces. When the adhesive bonding in the interface fails, the two concrete elements try to separate from each other. However, the reinforcement placed in tension will create a compression (clamping) force at the interface. This clamping force will act like an applied normal force and will cause a friction component to the resistance. In addition, the sliding of the elements will create bending stress in the reinforcement which leads to crushing of the concrete in the bending angle<sup>5</sup>.

When there is no reinforcement crossing the interface, the shear friction capacity will be achieved by the bonding strength between the two elements in contact and the frictional resistance force.

The curing condition of the joint material has also been suggested to influence the transfer of stresses between concrete surfaces<sup>6</sup>. Improper curing of the joint material can lead to excessive shrinkage, which will introduce a tensile stress between layers and can cause loss of adhesion and cracking at the interface prior to any load being applied. Cracking at the joint can also be caused by temperature deformations or stresses induced during construction (e.g. accidental dropping, twisting during placement, etc.)<sup>7</sup>.

#### TYPICAL TEST METHODS

There has been a significant amount of research previously conducted to evaluate the shear friction capacity of interfaces between dissimilar materials. Most of the experimental testing that has been conducted has included reinforcing steel crossing the shear plane. There are two principal test methods to evaluate the capacity in the interface: (1) push-off test, and (2) push-through test.

Even though the push-off test has not been standardized by ASTM, it is known as the most common test used by researchers in the evaluation of the shear friction capacity. Normally, the push-off test involves first casting an L-shaped specimen and allowing it to harden. This L-shaped specimen will have reinforcement to strengthen the L-shaped component itself and reinforcement that will cross the interface plane. After the first L-shaped component sufficiently hardens, the second L-shaped component is formed and cast. This second L-shaped component typically has the same geometry and reinforcement as the first L-shaped component. After the second L-shaped component is allowed to harden, the specimen is tested. A normal force can be applied perpendicular to the shear plane to provide a clamping force if desired. Most research that has been done using push-off tests used the same key steps, components, and characteristics, as shown in Fig 2.

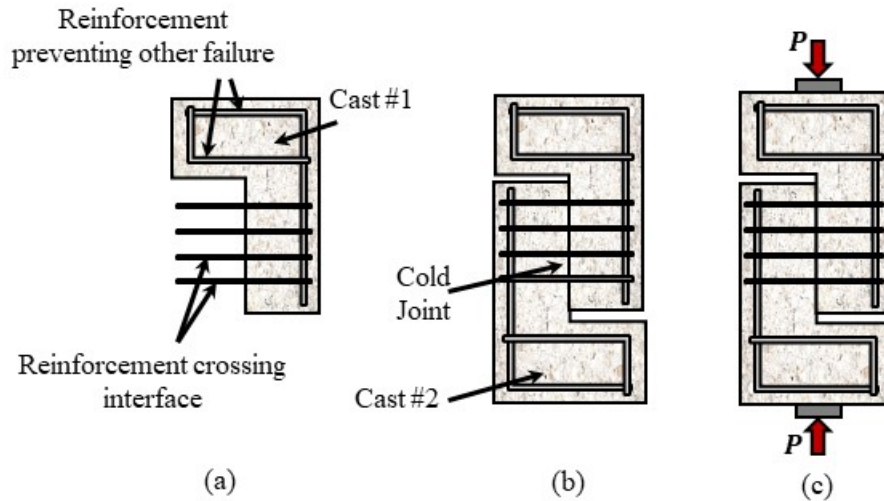


Fig 2: Typical casting and testing procedure for push-off tests: (a) casting of first L-shaped component, (b) casting of second L-shaped component, and (c) testing of push-off specimen.

The “push-through” test was proposed and used by Williams et al.<sup>8</sup> to evaluate both the shear friction capacity and the bond strength in the interface between two concrete cast at different times. The casting and testing procedure are similar to the push-off test, with the difference that in the push-through test two outer elements are cast at the same time and an inner element is then cast later directly between the other two elements, as shown in Fig 3. This test procedure also includes steel crossing the interface plane.

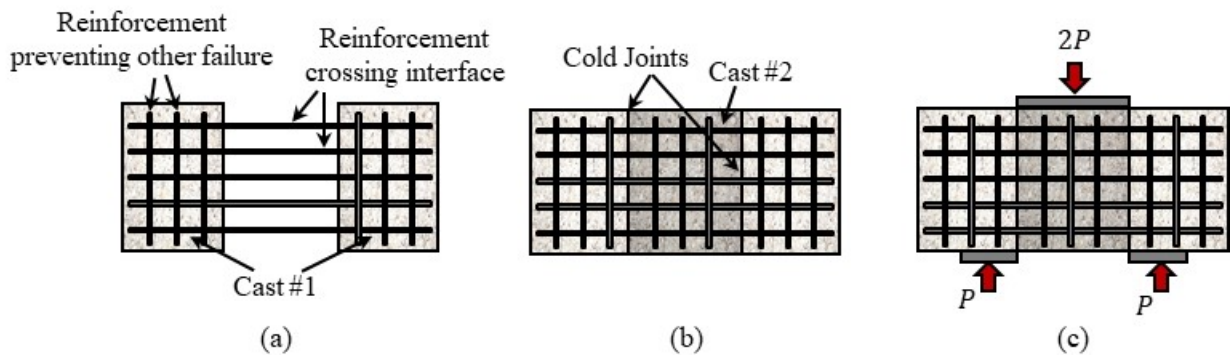


Fig 3: Typical casting and testing procedure for push-through test: (a) casting of outer elements, (b) casting of inner element, and (c) testing of the push-through specimen.

**PILE-TO-PILE CAP CONNECTIONS**

The required on-site connections between the elements often becomes a critical component of the overall bridge design. As PBES are being more widely used, more investigations and details on the connections have been developed to achieve monolithic behavior of the whole structure. The details of these connections vary depending on which elements are being

connected. The main objective of this project is to evaluate the connection between precast pile caps and piles.

There are two primary types of connections between these elements: pocket and socket connections, shown in Fig 4. Pocket connections are connections where the precast pile does not extend into the pocket in the precast pile cap, shown in Fig 4 (a). Reinforcement is extended from the precast pile into the pile cap and cast-in-place (CIP) concrete or grout is placed to fill the pocket, develop the reinforcement, and connect the two members. A corrugated metal pipe or duct is often used to form the void to enhance the bond between the CIP concrete or grout and the precast pile cap. Socket connections are connections where the precast pile is extended into a void in the pile cap and CIP grout or concrete is placed to connect the elements, shown in Fig 4 (b). Reinforcement can be included between the elements.

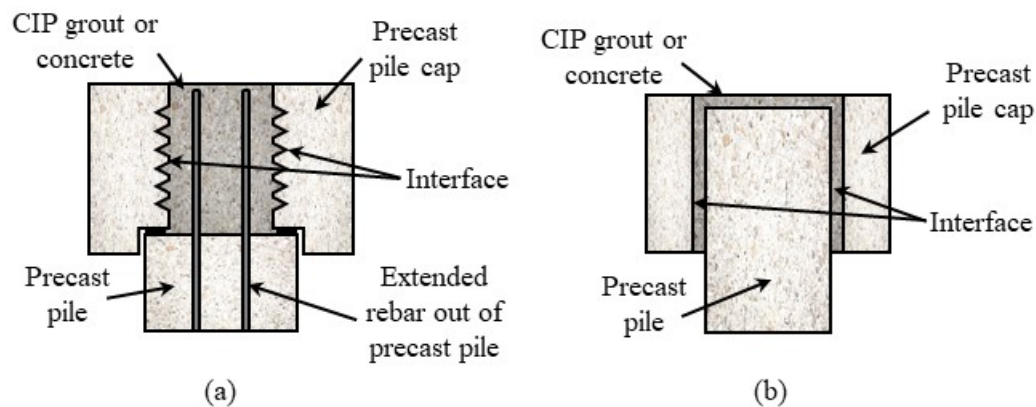


Fig 4: Example connection between pre-cast pile cap and pile: (a) pocket connection, and (b) socket connection.

The Florida Department of Transportation (FDOT) currently recommends a pocket connection between precast piles and precast pile caps. The precast pile cap is constructed with a void at the location of the pile that is slightly smaller than the piles and then placed on the driven piles. Reinforcement is then placed between the elements and the connection is filled with concrete to finish the connection. This connection detail relies partially on the bearing strength between the precast pile and precast pile cap and partially on the shear friction capacity between the CIP plug and the precast cap.

In this recommended connection there is no steel crossing the interface. This means that the shear friction component in this connection is made up of only the cohesion and interlock component of the CIP concrete (poured to finish the connection) to the surrounding material or precast element.

## PRELIMINARY TEST SPECIMENS

A first series of four specimens were cast to determine an appropriate test setup for the project and guide the development of the experimental matrix and future testing. Three different

geometries were used for these four specimens, shown in *Fig 5* and specified in *Table 1*. The dimensions were selected based on the available diameters of corrugated pipes.

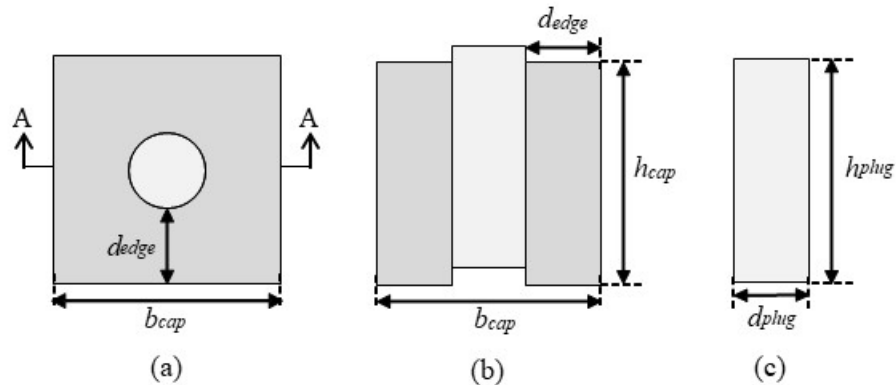


Fig 5: Specimen dimensions: (a) plan view, (b) section A-A, and (c) plug dimensions.

As shown in *Table 1*, the first three specimens (S1-1, S1-2, and S1-3) had varied geometries with an interface constructed using plastic corrugated pipe with a rib spacing of 2 inches, rib height of 7/8 inch and rib length of 1 inch. Plastic corrugated pipe was used so that it could be removed after casting of the cap and prior to casting of the plug. A corrugated metal pipe with rib spacing of 2 2/3 inches, rib height of 1/2 inch and rib length of 3/4 inch is typically used in pocket connections in the field. Future tests are being planned to determine the effect of the rib geometry and not removing the pipe.

Specimen S1-2 had half the overall height of S1-1, and specimen S1-3 was half the scale of S1-1, shown in Fig 6. Specimens S1-1 and S1-4 had the same geometry, but S1-4 had a smooth interface condition.

Table 1: Specimen dimensions details and specified material properties.

Specimen #	Pile Cap Dimensions (in)			Plug Dimensions (in)		Specified Concrete Strength	Yield Strength	Interface Condition
	$b_{cap}$	$w_{cap}$	$h_{cap}$	$d_{plug}$	$h_{plug}$			
S1-1	36	36	36	12	36	6.5 ksi	60 ksi	Corrugated
S1-2	36	36	18	12	18	6.5 ksi	60 ksi	Corrugated
S1-3	18	18	18	6	18	6.5 ksi	60 ksi	Corrugated
S1-4	36	36	36	12	36	6.5 ksi	60 ksi	Smooth

All of the Series 1 specimens had the same specified concrete compressive strength (6.5 ksi), interface surface preparation (as recommended by FDOT), plug and cap reinforcement scheme, and distance between the edge of plug and edge of cap ( $d_{edge}$  equal to  $d_{plug}$ ).

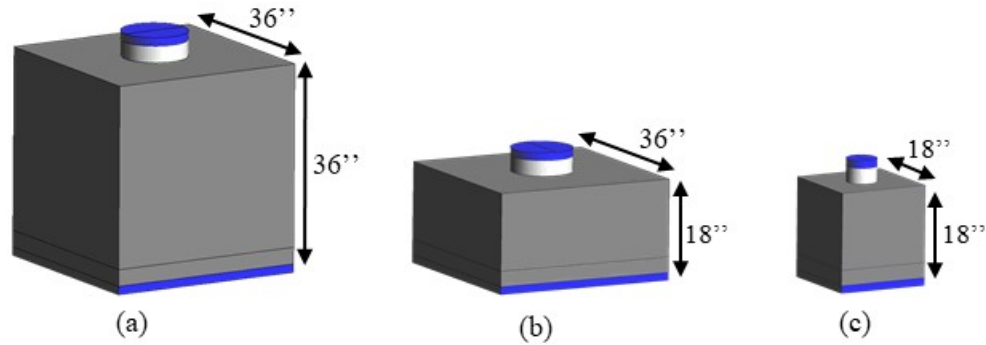


Fig 6: Dimensions of first series of specimens: (a) Specimens S1-1 and S1-4, (b) Specimen S1-2, and (c) Specimen S1-3.

### CONSTRUCTION PROCEDURE

A modified push-through test was envisioned for this project. An example of the proposed procedure for constructing the modified push-through test is as follows:

1. Cast 36" cube with a 12" diameter cylindrical void in the center. The cylindrical void was constructed using corrugated plastic pipe to vary the surface roughness.
2. Remove the corrugated plastic pipe used to create the internal void after the concrete has hardened. Sandblast surface of void to improve surface roughness.
3. Form a 12" diameter cylinder 3" above top face of cube and use 3" foam blockout at bottom of tube to create void at bottom. Place plug reinforcement and cast plug concrete.
4. Remove formwork and foam blockout after the concrete has hardened.

This procedure was followed for each of the specimens in Series 1 according to their specific dimensions. The proposed test specimens for the modified push-through are shown before and after casting of the center plug in Fig 7.

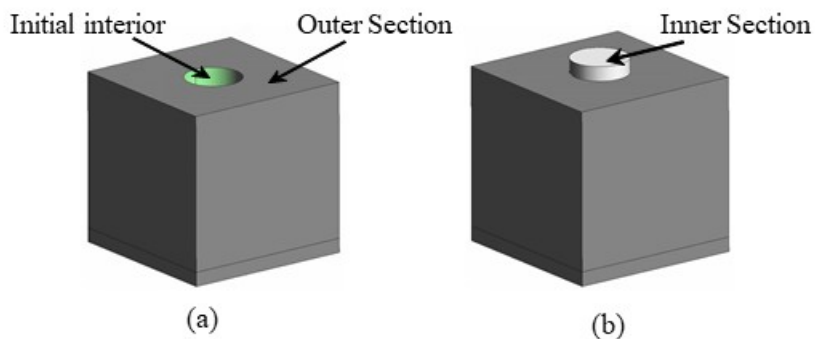


Fig 7: Proposed push-through test specimens: (a) casting of outer section, and (b) after casting the inner section.

## TEST SETUP

The test setup for the proposed modified push-through test is shown in Fig 8. The bottom of the test specimen was supported on two load blocks that were grouted to the ground. The load was applied using a hydraulic jack until failure of the interface or the capacity of the jack was reached. A 2-inch thick steel plate was used on top of the plug, as well as a thin layer of grout, for better distribution of the load over the surface. Two different section depths were used (18” and 36”) meaning the load frame needed to be adjusted between tests.

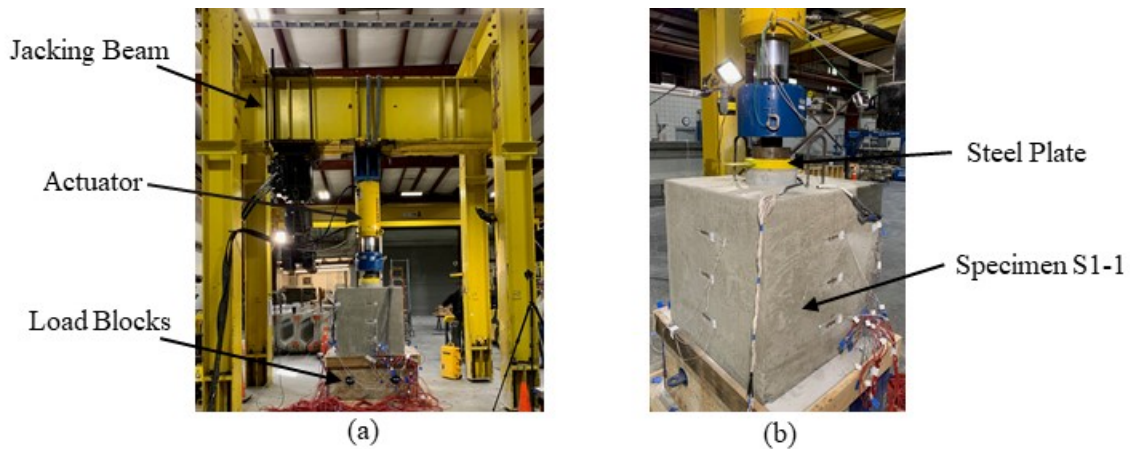


Fig 8: Test Sep-up for Specimens S1-1 and S1-4: (a) front view and (b) S-1Close-up

## ESTIMATED RESULTS

The capacity of these specimens was estimated using the current recommendations of AASHTO LRFD Bridge Design Specification<sup>9</sup> and finite element modeling.

### ESTIMATED STRENGTH USING AASHTO LRFD

There are several available procedures for estimating the shear friction capacity of a concrete structure or interface. Most of the current code expressions include components for a cohesion or aggregate interlock component as well as a contribution from steel crossing the friction plane or clamping force. The nominal shear capacity in the interface is found in the AASHTO LRFD Bridge Design Specification<sup>9</sup> as follow:

$$V_{ni} = cA_{cv} + \mu(A_{vf}f_y + P_c) \quad \text{Equation 1}$$

The capacity includes a concrete cohesion component ( $cA_{cv}$ ) and a friction component ( $\mu N$ ), where the normal force consists of the normal force from reinforcement perpendicular to the interface ( $A_{vf}f_y$ ) and any applied clamping force ( $P_c$ ). There are two limits on the nominal shear

friction capacity related to the concrete compression strength ( $f'_c$ ) and the area of the concrete interface plane ( $A_{cv}$ ), these limits were calculated for each specimen and the results are presented in Table 3.

None of the specimens had any steel reinforcement crossing the interface ( $A_{vf} = 0 \text{ in}^2$ ), and the finish of the surfaces were intentionally roughened (per the FDOT recommended finish). The interface condition was assumed to be “Normal weight concrete placed against a clean concrete surface, free of laitance, with surface intentionally roughened to an amplitude of 0.25 in”. All the parameters used to calculate the capacity of the interface for all specimens are shown in Table 2.

Table 2: Parameters used to calculate the shear friction capacity using AASHTO LRFD.

Specimen #	Cohesion Coefficient ( $c$ ) (ksi)	Friction Coefficient ( $\mu$ )	$K_1$	$K_2$ (ksi)	$A_{vf}$ ( $\text{in}^2$ )	$P_c$ (kips)	$f'_c$ (ksi)
S1-1	0.24	1.0	0.25	1.5	0	0	6.5
S1-2	0.24	1.0	0.25	1.5	0	0	6.5
S1-3	0.24	1.0	0.25	1.5	0	0	6.5
S1-4	0.24	1.0	0.25	1.5	0	0	6.5

The estimated capacity for all specimens were calculated following the procedure describe in the AASHTO LRFD Bridge Design Specifications<sup>9</sup>. The results are listed in Table 3.

Table 3: Estimated Capacity using AASHTO LRFD Bridge Design Specifications.

Specimen #	$A_{cv}$ ( $\text{in}^2$ )	$V_{ni}$ (kips)	$V_{ni}$ (kips)		Estimated Capacity $V_{ni}$ (kips)
			Limit 1	Limit 2	
S1-1	1,244	298.6	2,022	1,866	298.6
S1-2	565	135.7	919	848	135.7
S1-3	283	67.9	459	424	67.9
S1-4	1,244	298.6	2,022	1,866	298.6

#### ESTIMATED BEHAVIOR USING ATENA

Three main materials were defined to create the finite element models: concrete, reinforcement, and interface material. The parameters of the interface material were defined using the lower range values recommended by ATENA<sup>10</sup> and assigned to a volume element which is located between the pile cap and the plug. A summary of the material properties used for reinforcement and the interface is shown in Table 4.

Table 4: Material Characteristics used in ATENA to model the specimens.

	Variable	Input
<b>Reinforcement</b>	Young's Modulus (ksi)	29000
	Yield Strength (ksi)	60
<b>Interface Material</b>	Coefficient of Friction	0.3
	Tensile Strength (ksi)	0.0979
	Cohesion (ksi)	0.0979
	Min. Stiffness (kip/in <sup>3</sup> )	22.98
	Max. Stiffness (kip/in <sup>3</sup> )	22977

The concrete compressive strengths were measured on the day of testing for the pile cap and plug, shown in Table 5. The modulus of elasticity of the concrete was calculated based on the measured compressive strengths. The Poisson's ratio and tensile strength were based on recommendations for ATENA. The models were calibrated with these values to define the concrete material for the pile cap and the plug.

Table 5: Concrete Characteristics used model the specimens.

Specimen #	Compressive Strength on Test Day (ksi)		Young's Modulus (ksi)		Tension Strength (ksi)		Poisson's Ratio
	<i>Pile Cap</i>	<i>Plug</i>	<i>Pile Cap</i>	<i>Plug</i>	<i>Pile Cap</i>	<i>Plug</i>	
S1-1	7.57	8.45	4959	5330	0.435	0.449	0.20
S1-2	7.96	8.79	5098	5347	0.435	0.449	0.20
S1-3	7.69	8.20	5002	5162	0.435	0.449	0.20
S1-4	8.05	7.98	5098	5098	0.435	0.435	0.20

The estimated shear capacity of the interface and displacement at failure was found using all the parameters described above. The estimated capacity and displacement for all specimens are shown in Table 6. The same interface parameters were used for all these specimens (hence S1-1 has the same capacity as S1-4).

Table 6: Estimated shear friction capacity using ATENA software.

Specimen #	Estimated Capacity $V_{ni}$ (kips)	Displacement (in)
S1-1	388.03	0.10
S1-2	182.34	0.07
S1-3	175.37	0.23
S1-4	388.03	0.10

The cracking pattern and the load-displacement curve for Specimen S1-1 are shown in Fig 9. Significant cracking was predicted to develop vertically at mid-width of all the faces and micro-cracking radially around the top of the plug. The estimated behavior was that the specimen would have an approximately linear response up to the point when the cohesion was overcome. Then there would be a drop in load to the sustained load that could be held as sliding occurred along the interface. The software predicted a similar response in all specimens. Also note that the corrugations were not modeled in these preliminary models; modeling of the corrugations is currently being investigated.

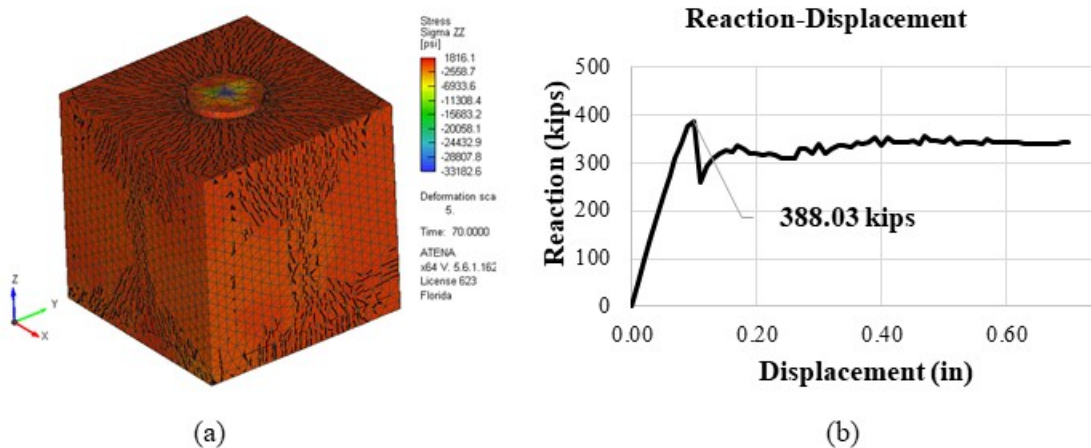


Fig 9: Summary of results for Specimen S1-1: (a) crack pattern at failure and (b) reaction-displacement curve.

## EXPERIMENTAL RESULTS

The results from the initial experimental testing of the first series of specimens are summarized in Table 7. The measured strengths were substantially larger than the estimated strengths using the current AASHTO LRFD Bridge Design Specification.

Table 7: Measured ultimate strength in experimental testing.

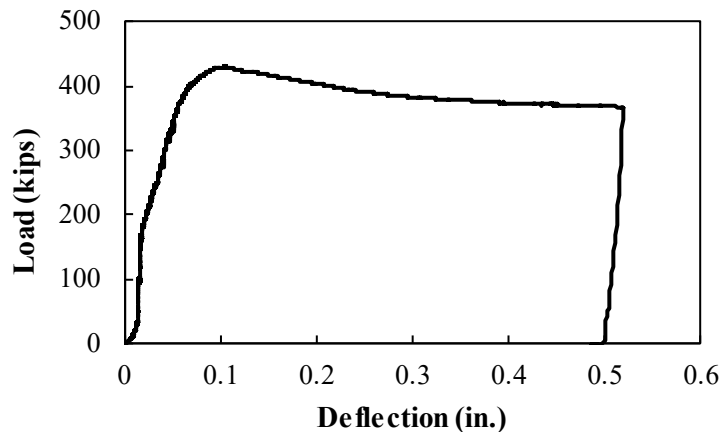
Specimen	Measured Strength ( $V_{n,measured}$ ) (kips)	$\frac{V_{ni,measured}}{V_{ni,AASHTO}}$
S1-1	> 750 kips	> 2.51
S1-2	> 750 kips	> 5.53
S1-3	243.8*	> 3.59
S1-4	429.7	1.44

\*failed due to crushing of concrete on top of plug

Specimen S1-1 had a corrugated interface between the plug and cap. The specimen was loaded to the capacity of the test setup (750 kips) but did not fail. Only minor displacement (0.06 inches at 750 kips) was observed. Specimen S1-2 had the same corrugated interface as Specimen 1 but had half of the overall height. This specimen was loaded to the capacity of the test setup (750 kips) but did not fail. Specimen S1-3 was half the scale of Specimen 1 with a similar corrugated interface between the cap and plug. The observed failure of this specimen was crushing of the concrete in the top of the plug at a load of 243.8 kips. Finally, Specimen S1-4 had the same geometry as Specimen S1-1, but had a smooth surface in the interface between the plug and cap. The observed failure for this specimen was a shear friction failure along the interface between the cap and plug. A linear response was observed until sliding of the plug began at a load of 429.7 kips, as shown in the load-deflection graph in Fig 10 and similar to the expected response from finite element modeling. Vertical cracking was only observed on two opposite sides of the specimens, shown in Fig 10 (a). The response of Specimen S1-4 would suggest that a splitting plane developed through the specimen, rather than evenly distributing radial stresses. Load was applied until the plug had slid 0.5 inch.



(a)



(b)

Fig 10: (a) Cracking at failure and (b) load versus deflection curve for Specimen S1-4.

## PRELIMINARY OBSERVATIONS AND FUTURE TESTING

Several preliminary observations can be made based on the initial experimental test results and numerical modeling:

1. The current procedure for estimating shear friction in the AASHTO LRFD Bridge Design Specification conservatively estimated the strength of these specimens. The smooth interface had a reasonable level of conservatism. The specimens with a corrugated interface had a large level of conservatism. This would suggest that the current procedure could be improved for estimating the shear friction capacity of this interface.
2. Loading of the plug causes tensile stresses to develop in a splitting plane across the cap at the location of the plug.
3. Dimensions of the corrugation related to the dimensions of the plug will impact the failure mechanism. The ribs in the corrugation used in preliminary testing were large compared to the plug diameter.

Future testing will be conducted to further investigate the effect of interface surface conditions, corrugation spacing and depth, presence of corrugation (removing versus leaving in place), edge distances, cap reinforcement, and concrete strength. Results will be used to make recommendations for improving the current procedure in the AASHTO LRFD Bridge Design Specification.

## REFERENCES

1. Rahal K. Shear-Transfer Strength of Reinforced Concrete. ACI Structural Journal. 2010;107(4):419.
2. International Federation for Structural Concrete (fib). fib Model Code 2010 Final draft, Volume 1. 2010.
3. Mohamad M, Ibrahim I, Abdullah R, Rahman A, Kueh A, Usman J. Friction and Cohesion Coefficients of Composite Concrete to Concrete Bond. Cement & Concrete Composites. 2015;56:1.
4. Randl N. Design Recommendations for Interface Shear Transfer in fib Model Code 2010. Structural Concrete. 2013;14(3):230.
5. Ali M, White R. Enhanced Contact Model for Shear Friction of Normal and High-Strength Concrete. ACI Structural Journal. 1999;96(3):348.
6. Santos P, Julio E, Silva V. Correlation Between Concrete to Concrete Bond Strength and the Roughness of the Substrate Surface. Construction and Building Materials. 2007;21(8):1688.
7. Mattock A, Hawkins N. Shear Transfer in Reinforced Concrete - Recent Research. PCI Journal. 1972;17(2):55.

8. Williams C, Massey J, Bayrak O, Jirsa J. Investigation of Interface Shear Transfer Using Push-Through Tests.
9. American Association of State Highway and Transportation Officials (AASHTO). AASHTO LRFD Bridge Design Specification, Customary U.S. Units, 6th Edition. Washington, D. C.; 2012.
10. Pryl D, Cervenka J. ATENA Program Documentation Part 11 - Troubleshooting Manual. 2017 p. 63.